CHEMISTRY
A EUROPEAN JOURNAL

DOI: 10.1002/chem.201001177

Mechanistic Insight into the Reactivity of Oxotransferases by Novel Asymmetric Dioxomolybdenum(VI) Model Complexes

Ramasamy Mayilmurugan,[a] Bastian N. Harum,[a] Manuel Volpe,[a] Alexander F. Sax,[b] Mallayan Palaniandavar,[c] and Nadia C. Mösch-Zanetti*[a]

Abstract: The asymmetric molybdenum(VI) dioxo complexes of the bis(phenolate) ligands 1,4-bis(2-hydroxybenzyl)-1,4-diazepane, 1,4-bis(2-hydroxy-4-methylbenzyl)-1,4-diazepane, 1,4-bis(2-hydroxy-3,5-dimethylbenzyl)-1,4-diazepane, 1,4-bis(2-hydroxy-3,5-di-*tert*-butylbenzyl)-1,4-diazepane, 1,4-bis(2-hydroxy-4-flurobenzyl)-1,4-diazepane, and 1,4-bis(2-hydroxy-4-chlorobenzyl)-1,4-diazepane (H_2(L1)–H_2(L6), respectively) have been isolated and studied as functional models for molybdenum oxotransferase enzymes. These complexes have been characterized as asymmetric complexes of type [MoO_2(L)] **1–6** by using NMR spectroscopy, mass spectrometry, elemental analysis, and electrochemical methods. The molecular structures of [MoO_2(L)] **1–4** have been successfully determined by single-crystal X-ray diffraction analyses, which show them to exhibit a distorted octahedral coordination geometry around molybdenum(VI) in an asymmetrical *cis*-β configuration. The Mo–O_{oxo} bond lengths differ only by ≈0.01 Å. Complexes **1**, **2**, **5**, and **6** exhibit two successive Mo^{VI}/Mo^{V} ($E_{1/2}$, −1.141 to −1.848 V) and Mo^{V}/Mo^{IV} ($E_{1/2}$, −1.531 to −2.114 V) redox processes. However, only the Mo^{VI}/Mo^{V} redox couple was observed for **3** and **4**, suggesting that the subsequent reduction of the molybdenum(V) species is difficult. Complexes **1**, **2**, **5**, and **6** elicit efficient catalytic oxygen-atom transfer (OAT) from dimethylsulfoxide (DMSO) to PMe_3 at 65 °C at a significantly faster rate than the symmetric molybdenum(VI) complexes of the analogous linear bis(phenolate) ligands known so far to exhibit OAT reactions at a higher temperature (130 °C). However, complexes **3** and **4** fail to perform the OAT reaction from DMSO to PMe_3 at 65 °C. DFT/B3LYP calculations on the OAT mechanism reveal a strong *trans* effect.

Keywords: asymmetric complexes · density functional calculations · electrochemistry · reaction mechanisms · structure–activity relationships · transferases

Introduction

Oxomolybdenum enzymes are ever-present in nature, and are involved in a variety of redox reactions, crucial in the metabolism of nitrogen, sulfur, and carbon compounds.[1–3] They catalyze controlled oxygen-atom-transfer (OAT) reactions coupled to electron transfer between a substrate and other cofactors such as iron–sulfur centers ([2Fe–2S] or [4Fe–4S]), hemes, or flavins.[4–6] These enzymes are commonly known as hydroxylases and oxotransferases, depending on whether the substrate is transferred by a primary oxygen-atom transfer or whether a water molecule is involved in substrate transformation. Many of these enzymes have been isolated from either obligate anaerobes or facultative anaerobes grown under anaerobic or microaerobic conditions. They have been classified into three broad families, xanthine oxidase (XO), sulfite oxidase (SO), and DMSO reductase (DMSOR), on the basis of the structure of their oxidized active centers.[6–9] They all consist of a mo-

[a] Dr. R. Mayilmurugan, B. N. Harum, Dr. M. Volpe, Prof. Dr. N. C. Mösch-Zanetti
Institut für Chemie, Bereich Anorganische Chemie
Karl-Franzens-Universität Graz
Schubertstrasse 1, 8010, Graz (Austria)
Fax: (+43) 316-380-9835
E-mail: nadia.moesch@uni-graz.at

[b] Prof. Dr. A. F. Sax
Institut für Chemie
Bereich Physikalische und Theoretische Chemie
Karl-Franzens-Universität Graz
Heinrichstrasse 28/VI, 8010, Graz (Austria)

[c] Prof. Dr. M. Palaniandavar
School of Chemistry, Bharathidasan University
Tiruchirappalli 620 024 (India)

Supporting information for this article is available on the WWW under http://dx.doi.org/10.1002/chem.201001177.

nonuclear molybdenum atom coordinated to one or two *cis*-dithiolene groups of pyranopterins (so-called molybdopterin), additional terminal oxo/hydroxo groups and/or sulfido groups, or side chains of serine, cysteine, selenocysteine, or aspartate residues in diverse coordination geometries.[3–6,9] The active sites of XO and DMSOR contain one oxo group in their oxidized forms which is transferred to the substrate. In contrast, SO consists of two oxo groups, of which only one is actually transferred. Thus, the five-coordinate square-pyramidal molybdenum atom is coordinated by two terminal oxo ligands at the equatorial and axial positions, an ene-1,2-dithiolate, and a catalytically essential Cys sulfur donor.[10–12] The more accessible equatorial oxo group is catalytically labile and positioned to be transferred to the substrate. On the other hand, the axial oxo group is less accessible to the substrate and acts as a spectator oxo group, and is believed to labilize the equatorial oxo ligand.[13] Recently, Enemark and co-workers reported the first spectroscopic evidence that in the SO enzyme the axial oxo ligand acts as a spectator, and that the equatorial oxo group is actually transferred.[14]

Bio-inspired dioxomolybdenum(VI) complexes have been prepared in great variety in recent years.[15] Close structural models represent dithiolene-based ligands,[16–21] but several oxomolybdenum complexes of non-dithiolene ligands, including pyridine dithiolates,[22,23] tris(pyrazolyl)borate ligands,[24] 3,5-*tert*-butyl-pyrazolate ligands,[25,26] β-ketiminates,[27,28] and bis(phenolate) ligands,[29–32] were also investigated. Furthermore, biomimetic models have been developed in order to investigate the influence of the spectator oxo effect on the OAT reaction. The first step in the OAT reaction is proposed to follow an associative mechanism, as demonstrated by Holm and co-workers in the OAT reaction between $[MoO_2(dithiolate)_2]^{2-}$ and tertiary phosphine using theoretical calculations.[33] Young and co-workers have found synthetic evidence for this proposal, as they were able to isolate and characterize crystallographically the adduct $[(LN_3)MoO(OPh)(OPEt_3)]$ (LN_3 trispyrazolyl borate) formed from the reaction of $[(LN_3)MoO_2(OPh)]$ and triethyl phosphine.[34] The adduct contains two distinct Mo–O distances (Mo=O, 1.684 (3); Mo–O···P, 2.157 (3) Å) resulting from substrate attack on the active oxo group followed by weakening of the Mo–O bond. The spectator oxo group forms a stronger Mo–O bond with triple-bond character, providing evidence for the spectator oxo effect described by Rappé and Goddard.[13] However, it is as yet unclear whether these structural changes have an impact on the OAT reactivity.

One possible approach for the investigation of the influence of the spectator oxo effect on the reactivity is the development of two molybdenum oxo compounds, one with and one without a spectator oxo ligand. Comparison of their reactivity towards OAT would allow the elucidation of the influence of the spectator oxo effect. However, the preparation of two such comparable compounds is challenging, because the substitution of the spectator oxo ligand in complexes with a $[MoO_2]^{2+}$ core by another doubly bonded group is either difficult to achieve (substitution by sulfido)[35] or also changes the sterical situation (substitution by imido),[27,36] preventing comparison on electronic grounds.

For this reason we envisioned the development of two ligand systems that exhibit very similar sterical constraints but allow the preparation of molybdenum dioxo compounds with asymmetric surroundings, and thus not identical molybdenum oxo bonds (with two different *trans* ligands), as well as symmetric surroundings with identical Mo–O bonds. Experimental and theoretical investigation of their OAT reactivities would allow us to elucidate whether the spectator oxo effect or the different *trans* effects govern the reactivity. We found such a pair of ligands in two bis(phenolate) systems that exhibit different linking nitrogen backbones, as shown here. Ligands H_2(L1)–H_2(L6) with the 1,4-diazepane

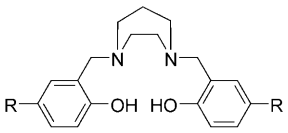

R = H, H_2(L1)
R = Me, H_2(L2)
R = F, H_2(L5)
R = Cl, H_2(L6)

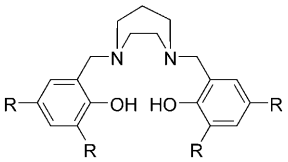

R = Me, H_2(L3)
R = *t*Bu, H_2(L4)

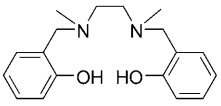

H_2(L7)

backbone lead to *cis*-β complexes, as recently shown in various iron complexes.[37,38] In contrast, ligand H_2(L7) with a 1,2-ethylenediamine linker leads to a *cis*-α molybdenum dioxo complex.[29]

Several molybdenum dioxo complexes with bis(phenolate) ligands of the salan type have been reported and found to be catalysts for various OAT reactions.[29–32,39] Recently, Britovsek, Gibson, and co-workers studied the electronic effects on oxygen atom transfer reactions between DMSO and PPh_3 at 130 °C using *cis*-dioxomolybdenum(VI) complexes of ethylenediamine-based bis(phenolate) ligands.[39] All reported systems were found to exhibit a symmetric coordination sphere about the metal center with two identical oxo groups (*cis*-α). To the best of our knowledge, asymmetric model complexes with salan-type ligands possessing non-identical oxo groups (*cis*-β) have not yet been reported, though an asymmetric arrangement is the most common in enzymes. Only very recently, a *cis*-β-$[MoO_2L]$ compound with an amine imine bis(phenolate) ligand was reported as a catalyst for hydrosilylation reactions.[40]

Here, we report the synthesis and crystallographic characterization of asymmetric molybdenum dioxo complexes containing 1,4-diazepane-based bis(phenolate) ligands. Their catalytic behaviors in the OAT reaction from DMSO to PMe_3 were investigated, and the complexes were found to

exhibit significantly higher activities compared to their symmetric analogues. Mechanistic aspects of the OAT reaction of both the asymmetric and symmetric complexes were established by means of DFT/B3LYP calculations.

Results and Discussion

Synthesis and characterization of ligands and complexes: The 1,4-diazepane-based ligands were synthesized according to known procedures,[41–43] which involve Mannich condensation and reductive amination, with suitable modifications as described in the Experimental Section. The amino hydrogen atoms in 1,4-diazepane were replaced with differently substituted phenol moieties to generate the ligands (Scheme 1) for the present study. Electron-withdrawing and electron-donating substituents were introduced, not only to tune the structural and electrochemical properties, but also to vary the reactivity of the model complexes.

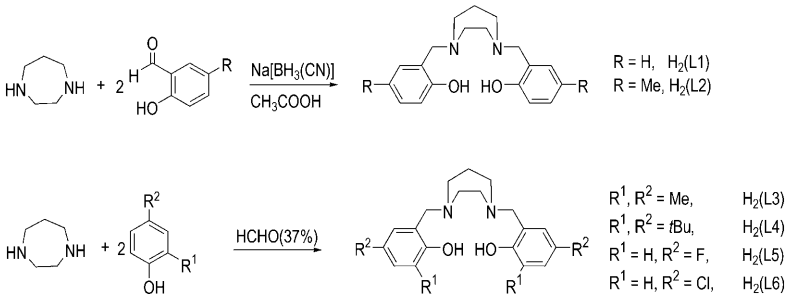

Scheme 1. Synthesis of bis(phenolate) ligands.

The reaction of $[MoO_2Cl_2]$ with the bis(phenolate) ligands H_2(L1)–H_2(L6) in the presence of two equivalents of Et_3N results in the formation of the asymmetric complexes **1**–**6** (Scheme 2). In contrast, the analogous reaction with the known bis(phenolate) ligand H_2(L7) yields the symmetric complex **7** (Scheme 2) as already described.[29] Complex formation was confirmed by ^{1}H NMR spectroscopy, as the two asymmetric protons of the methylene group give rise to four distinct doublets. In the free ligand, these methylene groups exhibit a characteristic singlet around 2.96–3.85 ppm in the ^{1}H NMR spectrum. The ^{19}F NMR spectrum of **5** shows two resonances of equal intensity at −122 and −126 ppm, indicating the asymmetric nature of the complex in solution. Furthermore, the general formula of the type $[MoO_2(L)]$ for all complexes **1**–**6** was confirmed by electron impact mass spectrometry and elemental analysis. Single-crystal X-ray diffraction analyses of compounds **1**–**4** (see below) confirm the structure shown in Scheme 2. The infrared spectra of all the dioxo compounds showed two strong bands around 880–887 and 910–18 cm^{-1}, corresponding to the asymmetric and symmetric Mo=O stretches, respectively.[44–46]

The dioxomolybdenum complexes **1**–**6** have good solubility in mixtures of acetonitrile and dichloromethane. However, their solubility in single common solvents varies with the electron-releasing and electron-withdrawing substituents on the phenyl rings. In general, complexes with *tert*-butyl/methyl substituents (**2**–**4**) are more soluble than those with electron-withdrawing substituents (**5**, −F; **6**, −Cl).

Molecular structures of 1–4: The X-ray crystal structures of **1**–**4** are shown in Figure 1 together with the numbering scheme for the donor atoms. Crystallographic details are given in Table 1, and selected bond lengths and bond angles are collected in Tables 2 and 3. Complexes **1**–**3** contain only one complex molecule in the asymmetric unit cell; complex **4** contains two crystallographically independent complex molecules with the same chemical formula and a free ligand molecule. All complex molecules **1**–**4** exhibit the same coordination geometry and configuration but slightly different bond lengths and bond angles. The molybdenum(VI) centers have a distorted octahedral MoN_2O_4 coordination sphere consisting of the two phenolate oxygen atoms and two tertiary amine nitrogen atoms of the bis(phenolate) ligand and two oxygen atoms from oxo groups occupying the remaining two

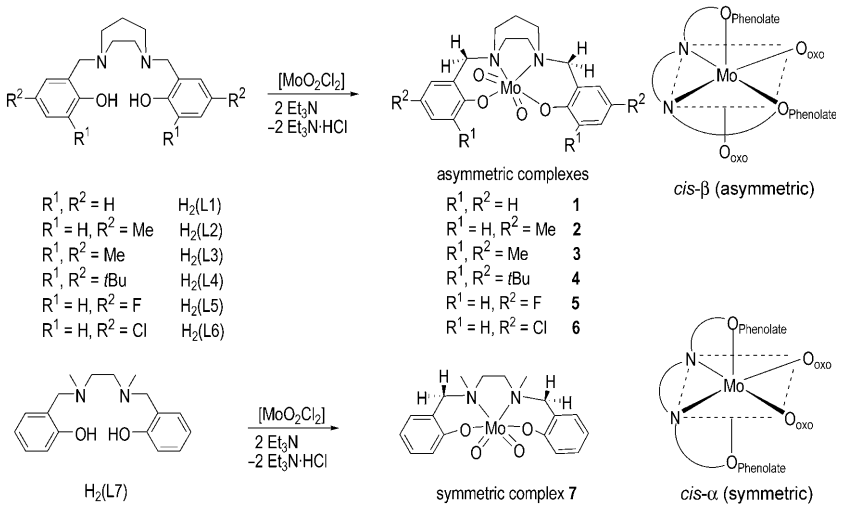

Scheme 2. Synthesis and geometrical configurations of dioxomolybdenum complexes.

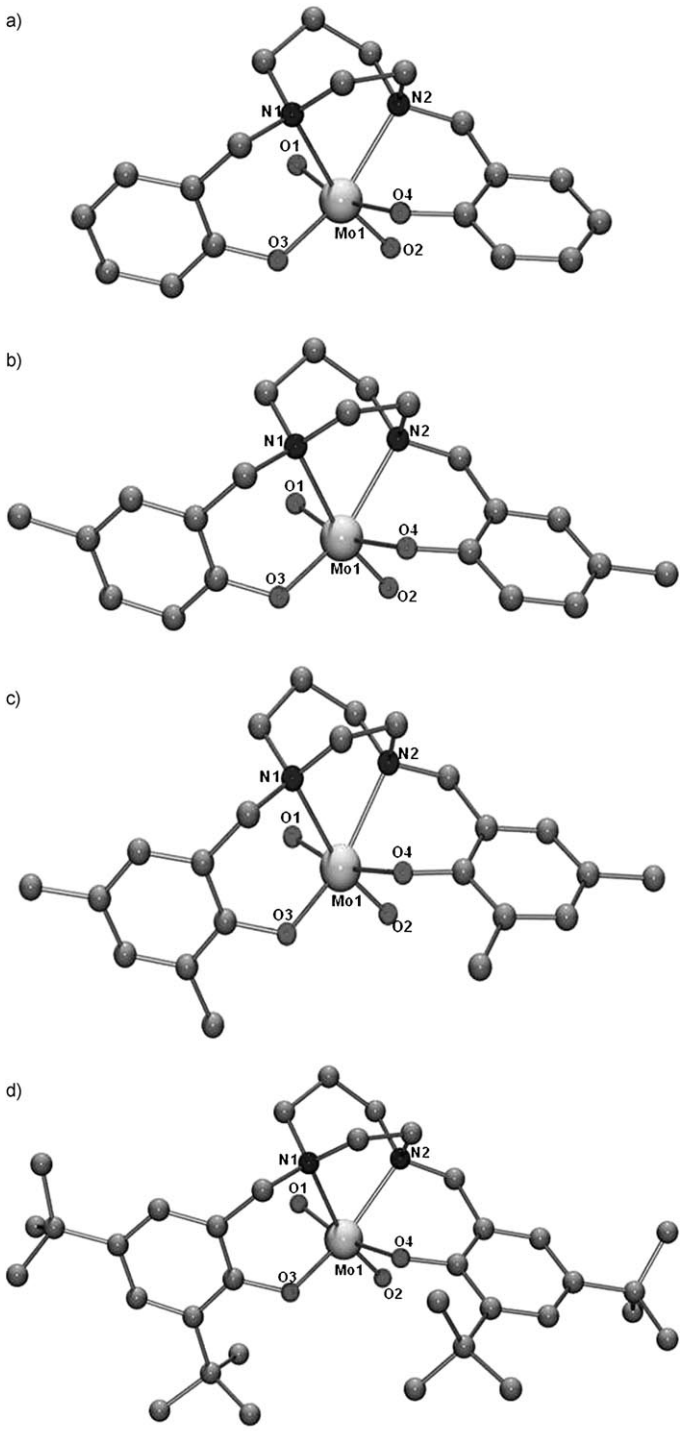

Figure 1. Molecular structure of complexes a) $[MoO_2(L1)]$ (**1**), b) $[MoO_2(L2)]$ (**2**), c) $[MoO_2(L3)]$ (**3**), d) $[MoO_2(L4)]$ (**4**) (50% probability factor for the thermal ellipsoid). Hydrogen atoms have been omitted for clarity.

coordination sites in a *cis*-β configuration (Scheme 2).[37,38] Thus, one of the phenolate oxygen atoms occupies a coordination site *trans* to an oxo group, and the other one is *cis* to an oxo group and *trans* to an amine nitrogen atom. The Mo–N bond *trans* to the oxo group is longer than the other Mo–N bond, which is *trans* to a phenolate oxygen atom. The $Mo–O_{phenolate}$ bond *trans* to the oxo group is also elongated compared to the other $Mo–O_{phenolate}$ bond, which is *trans* to the amine nitrogen atom. This is in agreement with a strong *trans* effect offered by the oxo group. The $Mo–O_{oxo}$ bond lengths are slightly asymmetric, differing only by ≈0.01 Å. The $Mo–O_{oxo}$ bond varies in length between 1.7061(9) and 1.7209(14) Å, which is in the normal for this type of bond in similar compounds reported in the literature.[29–32,39,44]

The Mo1–N1 bonds *trans* to the oxo group in the four compounds are very similar (**1** 2.423(3); **2** 2.4144(9); **3** 2.418(2); and **4** 2.4065(16) Å) and are slightly longer than in previously reported molybdenum complexes with bis(phenolate) ligands (≈2.38 Å).[29–32,39,44] The Mo1–N2 bonds *trans* to the phenolate oxygen atom are shorter, and decrease with electron-donating substituents at the phenolate ring (**1** 2.280(4); **2** 2.2657(9); **3** 2.264(2); and **4** 2.2537(16) Å). The same trend is observable in the Mo1–O3 and the Mo1–O4 bonds, for which the former ones *trans* to the amine (**1** 1.921(3); **2** 1.9295(9); **3** 1.9239(17); and **4** 1.9209(13) Å) are shorter than the latter ones *trans* to the oxo group (**1** 2.039(3); **2** 2.0507(9); **3** 2.0476(16); and **4** 2.0250(14) Å). It is interesting that the *cis*-β configuration of **1**–**4** is in contrast to the *cis*-α configuration of the analogous complex $[MoO_2(L7)]$ (**7**), in which $H_2(L7)$ is *N*,*N*′-dimethyl-*N*,*N*′-bis(2-hydroxybenzyl)-1,2-ethylenediamine and derivatives thereof.[29,39] Complex **7** and its derivatives have C_2 symmetry about an axis which passes through the molybdenum center and bisects the complex molecule. Thus, the $Mo–O_{oxo}$ bonds are equal in distance (≈1.70 Å), and are slightly shorter than those in **1**–**4** (1.7061(9)–1.7209(14) Å). Evidently, the steric constraints of the cyclic diamine backbone of $H_2(L1)$–$H_2(L6)$ do not appear to facilitate the disposition of the phenolate arms in the *trans* positions, and support the asymmetric *cis*-β configuration.

Redox properties: The redox behavior of the molybdenum(VI) complexes in a mixture of acetonitrile and dichloromethane (2:1) was studied by cyclic voltammetry (CV). Complexes **1**, **2**, **5**, and **6** exhibit two successive cathodic waves as well as their corresponding anodic waves (Table 4 and Supporting Information, Figure S1), which are assigned to the $Mo^{VI}\rightarrow Mo^{V}$ and $Mo^{V}\rightarrow Mo^{IV}$ redox processes, respectively.[29,31,47–49] However, complexes **3** and **4** show only one cathodic and one anodic wave (Table 4) corresponding to the $Mo^{VI}\rightarrow Mo^{V}$ redox process, but no well-defined Mo^{V}/Mo^{IV} redox couple was observed. The diffusion coefficients ($D = 0.3–3.5\times10^{-6}\,cm^2\,s^{-1}$ for Mo^{VI}/Mo^{V}; $0.2–6.5\times10^{-6}\,cm^2\,s^{-1}$ for Mo^{V}/Mo^{IV}) calculated by substituting the slope obtained from the linear i_{pc} versus $\nu^{1/2}$ ($\nu < 0.1\,V\,s^{-1}$) plot into the Randles–Sevcik equation[50] are of the same order as those observed for metal complexes undergoing two consecutive one-electron reduction processes.[31,37,39,41] The $E_{1/2}$ values of the Mo^{VI}/Mo^{V} redox potentials of the complexes from CV vary in the order **6** > **5** > **1** > **2** > **3** > **4** (Table 4), suggesting a decrease in Lewis acidity (ten-

Table 1. Crystallographic data and structure refinement for **1**–**4**.

	1	**2**	**3**	**4**
empirical formula	$C_{19}H_{22}MoN_2O_4$	$C_{21}H_{26}MoN_2O_4$	$C_{23}H_{30}MoN_2O_4$	$C_{109}H_{170}Mo_2N_8O_{10}$
M_r	438.33	466.38	494.43	1944.41
crystal system	monoclinic	monoclinic	monoclinic	triclinic
space group	*P*21/*c*	*P*21/*c*	*P*21/*c*	$P\bar{1}$
a[Å]	11.1207(7)	12.0414(9)	11.3989(5)	14.3956(11)
b [Å]	14.0465(9)	12.6870(9)	14.6030(6)	14.7574(12)
c [Å]	12.5162(8)	12.9491(9)	13.1437(6)	26.330(2)
α [°]	90	90	90	97.677(3)
β [°]	116.232(3)	96.505(3)	98.215(2)	93.908(4)
γ [°]	90	90	90	104.774(3)
V [Å^3]	1753.76(19)	1965.5(2)	2165.43(16)	5329.6(7)
T [K]	100(2)	100(2)	100(2)	100(2)
ρ_{calcd} [Mg m^{-3}]	1.660	1.576	1.517	1.212
Z	4	4	4	2
μ [mm^{-1}]	0.776	0.697	0.638	0.294
F(000)	896	960	1024	2088
reflns collected	20880	30505	67394	88673
goodness-of-fit on F^2	1.062	1.046	1.042	1.007
final *R1* [$I>2\sigma(I)$][a]	0.0446	0.0251	0.0327	0.0365
w*R*2 [$I>2\sigma(I)$][b]	0.0999	0.0634	0.0765	0.0759
R1 (all data)[a]	0.0631	0.0295	0.0458	0.0595
w*R*2 (all data)[b]	0.1083	0.0651	0.0809	0.0863

[a] $R1=\Sigma||F_o|-|F_c||/\Sigma|F_o|$; [b] $wR2=\Sigma w[(F_o^2-F_c^2)^2/\Sigma w[(F_o^2)^2]\}^{1/2}$.

Table 2. Selected bond lengths[a] [Å] and angles[a] [°] for **1**–**3**.

	1	**2**	**3**
Mo1−O1	1.720(3)	1.7172(9)	1.7194(16)
Mo1−O2	1.709(3)	1.7061(9)	1.7083(17)
Mo1−O3	1.921(3)	1.9295(9)	1.9239(17)
Mo1−O4	2.039(3)	2.0507(9)	2.0476(16)
Mo1−N1	2.423(3)	2.4144(9)	2.418(2)
Mo1−N2	2.280(4)	2.2657(9)	2.264(2)
O2-Mo1-O1	101.50(15)	100.36(5)	101.05(8)
O2-Mo1-O3	107.15(13)	108.28(4)	108.33(8)
O1-Mo1-O3	98.98(14)	98.35(4)	98.32(8)
O2-Mo1-O4	88.64(13)	88.20(4)	88.72(8)
O1-Mo1-O4	61.94(13)	162.01(4)	162.38(7)
O3-Mo1-O4	92.12(12)	93.85(4)	92.36(7)
O2-Mo1-N2	99.37(14)	99.16(4)	98.42(8)
O1-Mo1-N2	88.77(14)	87.75(4)	89.03(7)
O3-Mo1-N2	150.13(12)	150.18(4)	150.18(7)
O4-Mo1-N2	74.74(12)	75.20(3)	74.95(7)
O2-Mo1-N1	165.38(14)	165.87(4)	165.19(8)
O1-Mo1-N1	84.59(13)	83.68(4)	83.70(7)
O3-Mo1-N1	84.72(12)	84.29(4)	84.58(7)
O4-Mo1-N1	82.28(12)	84.44(3)	83.41(7)
N2-Mo1-N1	67.23(12)	67.30(3)	67.45(7)

[a] Standard deviations in parentheses.

Table 3. Selected bond lengths[a] [Å] and angles[a] [°] for **4**.

4a		**4b**	
Mo1−O1	1.7209(14)	Mo2−O5	1.7118(13)
Mo1−O2	1.7107(14)	Mo2−O6	1.7178(13)
Mo1−O3	1.9209(13)	Mo2−O7	1.9137(13)
Mo1−O4	2.0250(14)	Mo2−O8	2.0318(13)
Mo1−N1	2.4065(16)	Mo2−N3	2.4009(16)
Mo1−N2	2.2537(16)	Mo2−N4	2.2602(16)
O2-Mo1-O1	101.09(7)	O5-Mo2-O6	101.80(7)
O2-Mo1-O3	109.77(6)	O5-Mo2-O7	108.20(6)
O1-Mo1-O3	98.57(6)	O6-Mo2-O7	99.41(6)
O2-Mo1-O4	90.29(6)	O5-Mo2-O8	89.87(6)
O1-Mo1-O4	163.33(6)	O6-Mo2-O8	162.32(6)
O3-Mo1-O4	88.83(6)	O7-Mo2-O8	89.31(5)
O2-Mo1-N2	96.16(6)	O5-Mo2-N4	97.40(6)
O1-Mo1-N2	91.44(6)	O6-Mo2-N4	90.72(6)
O3-Mo1-N2	149.62(6)	O7-Mo2-N4	149.69(6)
O4-Mo1-N2	75.10(6)	O8-Mo2-N4	74.47(5)
O2-Mo1-N1	163.95(6)	O5-Mo2-N3	164.55(6)
O1-Mo1-N1	81.66(6)	O6-Mo2-N3	82.99(6)
O4-Mo1-N1	84.11(5)	O8-Mo2-N3	82.45(5)
N2-Mo1-N1	67.87(6)	N4-Mo2-N3	67.66(6)

[a] Standard deviations in parentheses; for complex **4**, two molecules were found in the unit cell: **4a** and **4b**.

methyl groups by more electron-releasing *tert*-butyl groups as in **4** ($E_{1/2}=-1.848$ V) the Mo^{VI}/Mo^{V} redox potential becomes more negative, also reflecting the decrease in Lewis acidity of the molybdenum center. This observation reveals that the electron-releasing methyl/*tert*-butyl groups on the phenolate arms in **2**–**4** decrease the tendency for reduction. Hence, the Mo^{V}/Mo^{IV} redox couples are not observed for **3** and **4**; the Mo^{V}/Mo^{IV} redox potentials are shifted to more negative values and possibly merge with the ligand reduction potential. However, the Mo^{VI}/Mo^{V} redox potential when employing phenolate ligands with electron-withdrawing groups as in **5** (−F) ($E_{1/2}=-1.189$ V) and **6** (−Cl) ($E_{1/2}=-1.141$ V) suggests the increase in Lewis acidity of the molybdenum(VI) center, as expected. Thus, the redox potentials of molybdenum(VI) centers are tuned by the electronic and steric factors of the phenolate donors. The plot of the Mo^{VI}/Mo^{V} redox potentials ($E_{1/2}$) versus the Hammett constant values (σ_p) for the *para* substituents in complexes **1**, **2**, **5**, and **6** is linear (Figure 2). This linear relationship indicates that the substituents at *para* position on the phenolate rings directly affect the electron density of the

dency to reduce) of the molybdenum(VI) center along this order. Furthermore, the $E_{1/2}$ values of Mo^{V}/Mo^{IV} redox potentials of the complexes also compile almost the same order: **6**>**5**>**2**>**1**. The Mo^{VI}/Mo^{V} redox potential of **1** ($E_{1/2}=-1.208$ V) is more positive than that of **2** ($E_{1/2}=-1.272$ V). This is in agreement with the electron-releasing nature of *p*-methyl groups decreasing the Lewis acidity and hence shifting the Mo^{VI}/Mo^{V} redox potential to more negative values. Further, upon incorporation of an additional methyl group in the *ortho*-position of the phenolate arms as in **3** ($E_{1/2}=-1.759$ V), and even more upon replacement of the

Table 4. Electrochemical data[a] for the Mo^{VI}/Mo^{V} and Mo^{V}/Mo^{IV} redox processes of molybdenum(VI) complexes in acetonitrile/dichloromethane solution[b] at room temperature, obtained using scan rates of 100 mV s^{-1} (CV).

Complex	E_{pc} [V]	E_{pa} [V]	ΔE_p [mV]	$E_{1/2}$ [V]	Redox process
1	−1.360	−1.057	303	−1.208	$Mo^{VI}\rightarrow Mo^{V}$
	−2.175	−2.053	122	−2.114	$Mo^{V}\rightarrow Mo^{IV}$
2	−1.439	−1.106	333	−1.272	$Mo^{VI}\rightarrow Mo^{V}$
	−1.882	−1.661	221	−1.771	$Mo^{V}\rightarrow Mo^{IV}$
3	−1.888	−1.630	258	−1.759	$Mo^{VI}\rightarrow Mo^{V}$
4	−2.025	−1.672	353	−1.848	$Mo^{VI}\rightarrow Mo^{V}$
	0.655	0.748	93	0.701	LO[c]
5	−1.294	−1.085	209	−1.189	$Mo^{VI}\rightarrow Mo^{V}$
	−1.712	−1.502	210	−1.607	$Mo^{V}\rightarrow Mo^{IV}$
6	−1.263	−1.019	244	−1.141	$Mo^{VI}\rightarrow Mo^{V}$
	−1.646	−1.416	230	−1.531	$Mo^{V}\rightarrow Mo^{IV}$

[a] Potential measured versus Ag/AgCl (0.01 M, 0.1 M NBu_4PF_6); add 0.544 V to convert to NHE. [b] CH_3CN/CH_2Cl_2 (2:1). [c] LO = ligand oxidation.

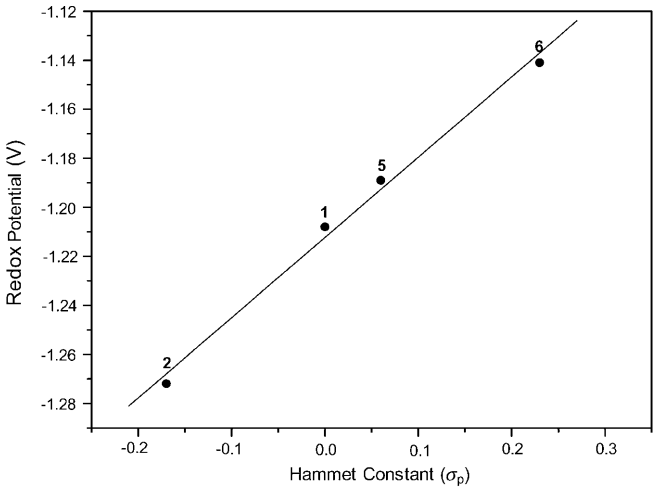

Figure 2. Plot of Mo^{VI}/Mo^{V} redox potentials ($E_{1/2}$) versus Hammett constant (σ_p) values for the *para* substituent in the complexes.

molybdenum center and hence the rate of OAT reactions.[31,39]

Oxygen-atom-transfer catalysis: Catalytic oxygen-atom transfer (OAT) between trimethylphosphine and excess dimethylsulfoxide (DMSO) using **1**, **2**, **5**, and **6** (10 mol% vs. PMe_3) as catalyst at 65 °C was investigated by ^{31}P NMR spectroscopy. After 1.5 to 3 h the PMe_3 was fully oxidized into O=PMe_3 (35.54 ppm) [Eq. (1)] when catalyzed by **1**, **5**, and **6**. However, more than 4 h were required with catalyst **2** for complete oxidation. Interestingly, complexes **3** and **4** failed to oxidize PMe_3. Their inactivity towards OAT reactions is presumably due not only to the higher Lewis basicity of the ligands $L3^{2-}$ and $L4^{2-}$, but also to increased steric hindrance. Furthermore, upon reaction of **4** with PMe_3 the bulky *tert*-butyl substituents on the ligand $L4^{2-}$ apparently weaken its coordination strength, as displacement from the coordination sphere is evident by the isolation of red crystals of the $[Mo_6O_{16}(PMe_3)_6]$ cluster (Figure S2 in the Supporting Information). The color of the solutions for **1**, **2**, **5**, and **6** remained yellow throughout the reaction, ruling out the formation of μ-oxo-dimolybdenum(V) or polynuclear molybdenum cluster complexes, which are usually purple or red.[51] The sterically hindered cyclic diazepane backbone in the present molybdenum(VI) complexes prevents the formation of more stable μ-oxo-dimolybdenum(V) complexes, which are involved in a general deactivation pathway in catalytic turnover.[51]

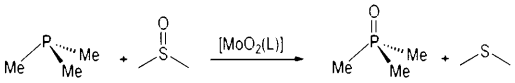

(1)

The pseudo-first-order rate constant k_{obs} of the OAT reaction between PMe_3 and DMSO catalyzed by 10 mol% of **1**, **2**, **5**, and **6** was determined as $k_{obs} = 4.51\times10^{-4}$, 6.20×10^{-5}, 7.01×10^{-4}, and 10.03×10^{-4} s^{-1} for **1**, **2**, **5**, and **6**, respectively (Figure S3 and Table S1 in the Supporting Information). In contrast to this, the replacement of the cyclic diazapane backbone by acyclic ethylenediamine led to a much slower OAT reaction. For example, under identical conditions using 10 mol% of **7**, only 18% transformation of PMe_3 into O=PMe_3 was observed over 3 h and we observed a k_{obs} of 3.10×10^{-5} s^{-1} (Figure S3 in the Supporting Information). We believe that in the complexes with the diazapane backbone the oxo group *trans* to the phenolate arm (Mo=O_{oxo} 1.720(3) Å) is catalytically labile and positioned to be transferred to the substrate. However, in **7** no such catalytically labile oxo group is present due to its symmetric *cis*-α configuration, which leads to two Mo=O bonds of equal length[29,39] and thus to a significant decrease of reactivity despite the similar steric surroundings of the two compounds. Comparison of the complexes **1**, **2**, **5**, and **6** reveals those with more electron-withdrawing groups (F and Cl) to have faster reaction rates. The plot of k_{obs} versus the Hammett constant values (σ_p) for the *para* substituents in complexes **1**, **2**, **5**, and **6** is linear (Figure 3). This confirms a nucleophilic attack of the phosphine on the metal oxo group. Furthermore, the linearity of the Hammett plot indicates the same reaction pathways in all investigated compounds.

DFT calculations: We were intrigued by the dramatic difference in reactivity. Thus, the OAT reaction from Me_2SO to PMe_3 for catalysts **1** and **7** was investigated by DFT studies in the gas phase (Figure 4). Further solution-phase calculations at selected stationary points using the COSMO model did not lead to a significant change in energy differences in comparison to the gas-phase calculations. The catalytic reaction involves two OAT steps: the first is from the catalyst $[MoO_2(L)]$ to the phosphine by an associative nucleophilic attack on the π* orbital of the weakly coordinated oxo group (Mo=O_{oxo} 1.720(3) Å) leading to a phosphine oxide coordinated intermediate[52] (**Int1**); and the second step is from the sulfoxide-coordinated compound $[MoO(L)(OSMe_2)]$ (**Int2**) to $[MoO(L)]$. The reaction from **Int1** to

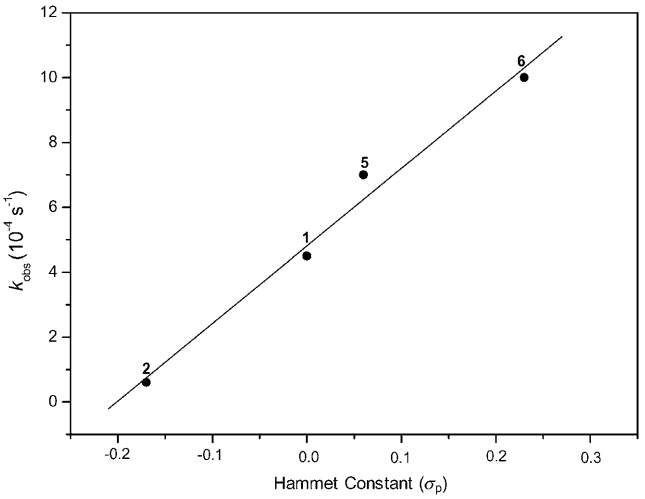

Figure 3. Plot of pseudo-first-order rate constants (k_{obs}) versus Hammett constant (σ_p) values for the *para* substituent in complexes.

Int2 represents the substitution of $OPMe_3$ by $OSMe_2$ via the transition state [MoO(L)] (**TS2**) by a dissociative mechanism.

The activation energy required for the first OAT step from the catalyst to the phosphine ([MoO(L)($OPMe_3$)] **TS1**), is very similar in both systems (87 kJ mol^{-1} for **1** and 78 kJ mol^{-1} for **7**). In the case of catalyst **1**, this activation energy is higher than those of the two following steps, thus rendering it the rate-determining step of the whole catalytic cycle. In contrast, for complex **7** the rate-determining step is found to be the substitution of $OPMe_3$ by $OSMe_2$ (activation energies 65 kJ mol^{-1} for **1** and 124 kJ mol^{-1} for **7**). To investigate this difference further we analyzed the bonding situation in **Int1**. The Mo–O bond in Mo–O=P is significantly stronger in [MoO(L7)($OPMe_3$)] (2.18 Å) than in [MoO(L1)-($OPMe_3$)] (2.32 Å). This can be explained by the structural difference between compounds **1** and **7**. The former contains two different oxo atoms, where OAT occurs preferentially from the oxo group in *trans* position to the phenolate oxygen. The attack of the oxo group *trans* to the amine was found to be higher in energy. In the case of **7**, however, both oxo groups are electronically equivalent and are in *trans* position to the amines. The higher *trans* influence of the phenolate oxygen versus the amine nitrogen atom weakens the molybdenum oxo bond, and thereby decreases the activation energy of the substitution. The molybdenum oxo bond length of the spectator oxo group remains constant in both compounds throughout the reaction pathway, which suggests the absence of a spectator oxo effect. This is a strong indication that the large reactivity difference is caused mainly by different *trans* effects.

Conclusion

Asymmetric dioxomolybdenum complexes of new bis(phenolate) ligands with diazepane backbones have been isolated and studied as structural and functional models for oxo-transferring molybdoenzymes. These complexes exhibit a distorted octahedral molybdenum(VI) coordination geometry with an unusual asymmetric *cis*-β configuration. The asymmetric Mo^{VI}–O_{oxo} bond lengths are in contrast to the symmetric Mo^{VI}–O_{oxo} bond found in the ethylenediamine analogue with *cis*-α configuration. The present molybdenum(VI) complexes with simple electron-withdrawing substituents on the phenolate catalyze the biologically relevant oxygen atom transfer between DMSO and PMe_3 efficiently by a nucleophilic attack of the phosphine on the metal oxo group. In contrast, the analogous bis(methyl/*tert*-butylphenolate) complexes are inactive towards the OAT reactions due to the decreased Lewis acidity of the molybdenum(VI) center and its steric hindrance conferred by the electron-releasing methyl/*tert*-butyl groups on the phenolate rings. The efficient oxygen transfer of the present complexes depends

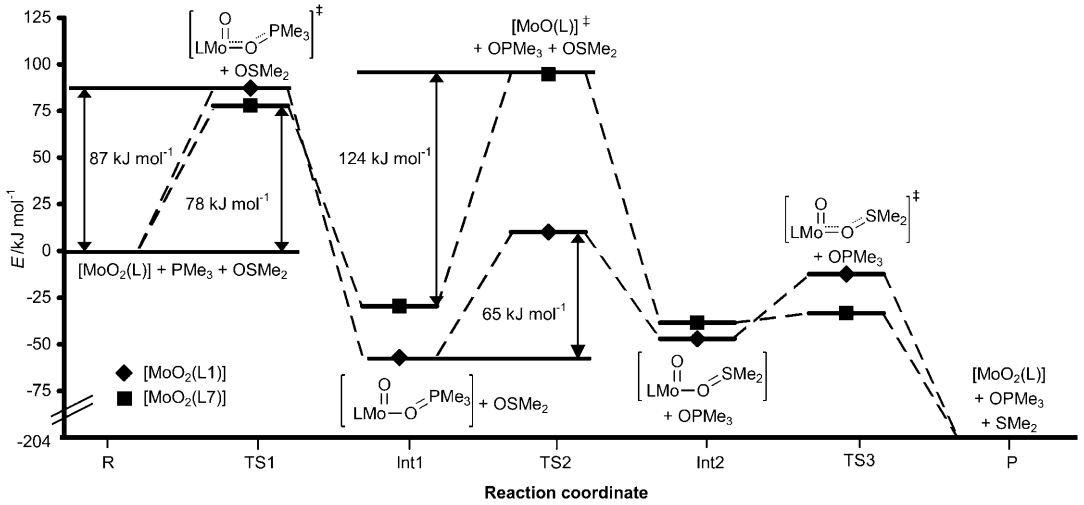

Figure 4. Energy profile for OAT from DMSO to PMe_3 catalyzed by **1** and **7**. Energies are given in kJ mol^{-1} relative to the reactants at the B3LYP def2-SVP level of theory.

strongly upon the ligand architecture fine-tuned by the nature of the substituents on the phenolate rings, and also on the geometrical configuration around the molybdenum center. The huge difference in OAT reactivity determined experimentally for the sterically similar compounds **1** and **7** can be related to the different *trans* effects of the phenolate oxygen compared to the amine nitrogen atoms, but, as evidenced by DFT calculations, cannot be attributed to a spectator oxo effect.

Experimental Section

Materials: Homopiperazine, 2-hydroxy-5-methylbenzaldehyde, 2,4-dimethylphenol, 2,4-di-*tert*-butylphenol, sodium cyanotrihydroborate, $[MoO_2Cl_2]$ (Aldrich), 4-flurophenol, 4-chlorophenol, 37% aqueous formaldehyde, 2-hydroxybenzaldehyde, and *N,N′*-dimethylethylenediamine were used as received, unless noted otherwise. The ligand *N,N′*-dimethyl-*N,N′*-bis(2-hydroxybenzyl)ethylenediamine (H_2(L7)) and its dioxomolybdenum(VI) complex $[MoO_2(L7)]$ (**7**) were synthesized as described previously.[29] All deuterated solvents were purchased from Deutero GmbH and dried over molecular sieves. All solvents were dried by a solvent purification system from Innovative Technology inc. and flushed with argon prior to use. Celite and aluminum oxide were purchased from commercial sources and dried in vacuo at 300 °C. The supporting electrolyte, $[NBu_4]PF_6$, was purified, dried under vacuum for 48 h at 100 °C, then kept under N_2 in the glove box.

Experimental conditions and physical measurements: The manipulations were carried out under dry argon using standard Schlenk line or glove box techniques for the reactions involving air-sensitive compounds. All NMR spectra were recorded at 360 MHz on a Bruker AMX 360 spectrometer. Chemical shift values are given in parts per million (ppm). Electron impact mass spectra were measured on an Agilent 5973 MSD-Direct Probe. Elemental analyses were carried out using a Heraeus Vario Elementar automatic analyzer at the Institute of Inorganic Chemistry, Graz University of Technology, Austria. IR spectra were recorded with a Perkin–Elmer 1725X FTIR spectrometer. Cyclic voltammetry (CV) was performed in a glove box using a three-electrode cell configuration. A platinum disc, a platinum wire, and $Ag(s)/Ag^+$ were used as the working, auxiliary, and reference electrodes, respectively, and NBu_4PF_6 was used as the supporting electrolyte. The $E_{1/2}$ values were observed under identical conditions for various scan rates. The instruments utilized included a GAMRY Potentiostat/Galvanostat and GAMRY-framework software to carry out the experiments and to acquire the data.

Synthesis of ligands: The ligands 1,4-bis(2-hydroxybenzyl)-1,4-diazepane, H_2(L1), and 1,4-Bis(2-hydroxy-3,5-di-*tert*-butylbenzyl)-1,4-diazepane, H_2(L4), were synthesized and purified as previously reported.[41]

1,4-Bis(2-hydroxy-4-methylbenzyl)-1,4-diazepane (H_2(L2)): Homopiperazine (0.50 g, 5.0 mmol) and a small amount of acetic acid were added to a solution of 2-hydroxy-5-methylbenzaldehyde (1.36 g, 10.0 mmol) in methanol (50 mL). Sodium cyanotrihydroborate (0.63 g, 10.0 mmol) in methanol (5 mL) was added dropwise to the resulting solution with stirring. After the solution had been stirred for three days at 25 °C, it was acidified by adding concd HCl and then evaporated almost to dryness under reduced pressure. The residue was dissolved in saturated aqueous Na_2CO_3 solution (50 mL) and extracted with $CHCl_3$ (3×50 mL). The combined extracts were dried over anhydrous Na_2SO_4 and filtered. Slow evaporation of the filtrate gave the white crystalline ligand H_2(L2). Yield: 0.84 g (49%). The ligand was further purified by recrystallization from CH_2Cl_2. ^{1}H NMR (360 MHz, C_6D_6): δ = 1.28 (m, 2H), 2.14 (s, 6H), 2.16 (s, 4H), 2.21 (t, J = 6.08 Hz, 4H), 3.24 (s, 4H), 6.59 (d, J = 2.34 Hz, 2H), 6.92–7.15 ppm (m, 4H); ^{13}C NMR (360 MHz, C_6D_6): δ = 20.91 (CH_3), 27.06, 53.50, 54.81, 62.28 (CH_2), 116.86, 122.29, 128.20, 129.74, 130.07, 156.97 ppm (ArC).

1,4-Bis(2-hydroxy-3,5-dimethylbenzyl)-1,4-diazepane (H_2(L3)): A solution of 2,4-dimethylphenol (3.66 g, 30.0 mmol), homopiperazine (1.50 g, 15.0 mmol) and 37% aqueous formaldehyde (3.5 mL, 42.0 mmol) in methanol (10 mL) was stirred under reflux conditions for 24 h. The mixture was cooled and the product obtained was filtered off and washed with ice-cold methanol to give a colorless product. Yield: 4.20 g (76%). The product was purified by recrystallization from CH_2Cl_2. ^{1}H NMR (360 MHz, $CDCl_3$): δ = 1.89 (m, 2H), 2.17 (s, 12H), 2.74 (s, 4H), 2.79 (t, J = 6.07 Hz, 4H), 3.70 (s, 4H), 6.83 (s, 2H), 6.58 (s, 2H), 7.23 ppm (s, 2H); ^{13}C NMR (360 MHz, $CDCl_3$): δ = 15.56, 20.34 (CH_3), 26.46, 53.37, 54.36, 61.72 (CH_2), 120.63, 124.60, 126.61, 127.61, 130.62, 153.51 ppm (ArC).

1,4-Bis(2-hydroxy-4-fluorobenzyl)-1,4-diazepane (H_2(L5)): Aqueous formaldehyde (37%) (3.5 mL, 45.4 mmol) was added to a stirred solution of homopiperazine (1.13 g, 11.3 mmol) and 4-fluorophenol (3.93 g, 22.7 mmol) in methanol (50 mL). The mixture was heated under reflux for 12 h and then cooled to room temperature. The white precipitate was filtered off, washed with cold methanol, and dried under vacuum to yield a white powder (0.44 g, 11%). ^{1}H NMR (300 MHz, C_6D_6): δ = 1.18 (m, 1H), 1.98 (s, 4H), 2.06 (t, J = 6.05 Hz, 4H), 2.99 (s, 4H), 6.48–6.50 (m, 2H), 6.72–6.87 ppm (m, 4H); ^{13}C NMR (360 MHz, C_6D_6): δ = 29.20, 52.74, 53.83 (CH_2), 61.0 (d, J_{C-F} = 1.38 Hz, -CH_2), 115.0 (dd, J_{C-F} = 12.03, 22.82 Hz, ArC), 117.0 (d, J_{C-F} = 7.70 Hz, ArC), 122.7 (d, J_{C-F} = 6.83 Hz, ArC), 154.4 (d, J_{C-F} = 1.93 Hz, ArC), 154.57, 157.70 ppm (ArC); ^{19}F NMR (360 MHz, $CDCl_3$): δ = −125 ppm (2F; ArF).

1,4-Bis(2-hydroxy-4-chlorobenzyl)-1,4-diazepane (H_2(L6)): This ligand was prepared as described above for H_2(L5), except that 4-chlorophenol (2.54 g, 11.3 mmol) was used instead of 4-fluorophenol to yield a white powder (0.529 g, 14%). ^{1}H NMR (300 MHz, C_6D_6): δ = 1.15 (m, 1H), 1.92 (s, 4H), 2.0 (t, J = 6.06 Hz, 4H), 2.96 (s, 4H), 6.75–6.82 (m, 4H), 7.01–7.15 ppm (m, 2H); ^{13}C NMR (360 MHz, C_6D_6): δ = 26.44, 53.05, 53.97, 61.12 (CH_2), 117.94, 123.59, 123.86, 128.62, 129.12, 157.43 ppm (ArC).

Synthesis of complexes—general procedure: The complexes $[MoO_2(L1)]$ (**1**) to $[MoO_2(L6)]$ (**6**) were prepared by reaction of a solution of $[MoO_2Cl_2]$ (0.198 g, 1.0 mmol) in acetonitrile (10 mL) with a solution of the respective ligand H_2(L) (1.0 mmol) in acetonitrile (10 mL), in the presence of two equivalents of triethylamine (Et_3N) (0.20 g, 280 μL, 2.0 mmol). The solution was stirred, and a yellow precipitate was obtained, which was filtered, washed with small amounts of acetonitrile, and dried in vacuo.

$[MoO_2(L1)]$ (1): The crude complex was thoroughly washed with pentane to remove any residual free ligand. Then the complex was redissolved in a mixture of acetonitrile and dichloromethane and filtered over a pad of Celite. Removal of the solvent in vacuo yielded the yellow complex **1**. Yield: 0.28 g (64%); ^{1}H NMR (360 MHz, $CDCl_3$): δ = 1.25 (m, 2H; -CH_2-), 1.41 (t, J_{HH} = 7.33 Hz, 1H; -CH_2-N), 1.97 (m, 1H; -CH_2-N), 2.32 (m, 1H; -CH_2-N), 2.50 (dd, J_{HH} = 7.34 Hz, 1H; -CH_2-N), 3.40 (d, J_{HH} = 12.17 Hz, 1H; Ar-CH_2-N), 3.60 (d, J_{HH} = 14.48 Hz, 2H; Ar-CH_2-N, -CH_2-N), 3.76 (m, 1H; -CH_2-N), 3.99 (m, 1H; -CH_2-N), 4.20 (d, J_{HH} = 12.09 Hz, 1H; Ar-CH_2-N), 4.37 (m, 1H; -CH_2-N), 4.70 (d, J_{HH} = 14.47 Hz, 1H; Ar-CH_2-N), 6.73–7.35 ppm (m, 8H; ArH); MS (EI): *m/z* (%): 440 (100) $[M]^+$; IR (KBr; Mo=O): $\tilde{\nu}$ = 883 (s), 912 cm^{-1} (s); elemental analysis calcd (%) for $C_{19}H_{22}MoN_2O_4$: C 52.06, H 5.06, N 6.39; found: C 51.87, H 5.13, N 6.38; single crystals suitable for X-ray diffraction analysis were grown by diffusion of diethyl ether into a solution of complex **1** in dichloromethane.

$[MoO_2(L2)]$ (2): The yellow solid was thoroughly washed with pentane to remove any residual free ligand. Then the complex was redissolved in a mixture of acetonitrile and dichloromethane and layered with diethyl ether to obtain yellow crystals of compound **2**. Yield: 0.24 g (52%); ^{1}H NMR (360 MHz, $CDCl_3$): δ = 1.93 (m, 2H; -CH_2-), 2.22 (s, 2H; -CH_2-N), 2.24 (s, 3H; Ar-*p*-CH_3), 2.30 (s, 3H; Ar-*p*-CH_3), 3.08 (m, 1H; -CH_2-N), 3.30 (d, J_{HH} = 12.12 Hz, 1H; Ar-CH_2-N), 3.60 (d, J_{HH} = 14.59 Hz, 1H; Ar-CH_2-N), 3.64 (m, 1H; -CH_2-N), 3.74 (m, 2H; -CH_2-N), 4.0 (m, 1H; -CH_2-N), 4.20 (d, J_{HH} = 12.08 Hz, 1H; Ar-CH_2-N), 4.30 (m, 1H; -CH_2-N), 4.60 (d, J_{HH} = 14.47 Hz, 1H; Ar-CH_2-N), 6.70–6.98 ppm (m, 6H; ArH); MS (EI): *m/z* (%): 468 (100) $[M]^+$; IR (KBr; Mo=O): $\tilde{\nu}$ = 887 (s),

914 cm^{-1} (s); elemental analysis calcd (%) for $C_{21}H_{26}MoN_2O_4$: C 54.08, H 5.62, N 6.01; found: C 53.18, H 5.80, N 6.01; single crystals suitable for X-ray diffraction analysis were obtained from a solution of complex **2** in acetonitrile at room temperature.

[MoO_2(L3)] (3): The yellow solid was thoroughly washed with pentane to remove any residual free ligand. Then, the by-product $Et_3N{\cdot}HCl$ was precipitated by dissolving the complex in a small amount of THF, and the solution was filtered over a pad of Celite. Removal of the solvent in vacuo yielded the pure yellow complex **3**. Yield: 0.30 g (61%); ^{1}H NMR (360 MHz, $CDCl_3$): δ = 1.85 (m, 2H; -CH_2-), 1.97 (m, 1H; -CH_2-N), 2.09 (s, 3H; CH_3), 2.20 (s, 3H; CH_3), 2.26 (s, 3H; CH_3), 2.28 (s, 3H; CH_3), 2.60 (m, 3H; -CH_2-N), 2.78 (m, 1H; -CH_2-N), 3.51–3.62 (m, 2H; -CH_2-N, Ar-CH_2-N), 4.05 (m, 1H; -CH_2-N), 4.39 (m, 1H; -CH_2-N), 4.57 (d, J_{HH} = 14.43 Hz, 1H; Ar-CH_2-N), 6.53 (s, 1H; Ar-H), 6.79 (s, 1H; Ar-H), 6.86 (s, 1H; Ar-H), 7.01 ppm (s, 1H; Ar-H); MS (EI): *m/z* (%): 496 (100) $[M]^+$; IR (KBr; Mo=O): $\tilde{\nu}$ = 883 (s), 918 cm^{-1} (s); elemental analysis calcd (%) for $C_{23}H_{30}MoN_2O_4$: C 55.87, H 6.12, N 5.67; found: C 56.46, H 6.21, N 5.60; single crystals suitable for X-ray diffraction analysis were grown by diffusion of diethyl ether into a solution of complex **3** in dichloromethane.

[MoO_2(L4)] (4): The complex was purified in an analogous manner to **3**, and the yield was 0.34 g (51%). ^{1}H NMR (360 MHz, $CDCl_3$): δ = 1.20 (m, 2H; -CH_2-), 1.36 (s, 9H; *t*Bu), 1.40 (s, 9H; *t*Bu), 1.44 (m, 2H; -CH_2-N), 1.61 (s, 9H; *t*Bu), 1.84 (s, 9H; *t*Bu), 1.97 (t, J = 6.53 Hz, 2H; -CH_2-N), 2.70 (d, J_{HH} = 12.02 Hz, 2H; Ar-CH_2-N), 3.0 (d, J_{HH} = 14.47 Hz, 2H; Ar-CH_2-N), 3.10 (m, 1H; -CH_2-N), 3.33 (m, 1H; -CH_2-N), 3.60 (m, 3H; -CH_2-N), 3.91 (d, J_{HH} = 11.95 Hz, 2H; Ar-CH_2-N), 4.30 (m, 1H; -CH_2-N), 4.40 (d, J_{HH} = 14.36 Hz, 2H; Ar-CH_2-N), 6.80 (d, J_{HH} = 2.22 Hz, 1H; Ar-H), 6.99 (d, J_{HH} = 2.34 Hz, 1H; Ar-H), 7.60 ppm (m, 2H; Ar-H); MS (EI): *m/z* (%): 664 (100) $[M]^+$; IR (KBr; Mo=O): $\tilde{\nu}$ = 884 (s), 918 cm^{-1} (s); elemental analysis calcd (%) for $MoC_{35}H_{54}N_2O_4$: C 63.43, H 8.21, N 4.23; found: C 62.81, H 8.14, N 4.32; X-ray quality crystals were obtained by slow evaporation of the reaction solution in inert atmosphere at room temperature.

[MoO_2(L5)] (5): The yellow solid was thoroughly washed with toluene and acetonitrile and dried in vacuo to yield yellow complex **5**. Yield, 0.22 g (47%). ^{1}H NMR (360 MHz, $CDCl_3$): δ = 1.26 (m, 2H; -CH_2-), 1.94 (m, 1H; -CH_2-N), 2.37 (m, 1H; -CH_2-N), 2.57 (m, 1H; -CH_2-N), 3.40 (d, J_{HH} = 12.48 Hz, 1H; Ar-CH_2-N), 3.60 (d, J_{HH} = 14.87 Hz, 1H; Ar-CH_2-N), 3.70 (m, 1H; -CH_2-N), 3.73 (m, 1H; -CH_2-N), 3.77 (m, 2H; -CH_2-N), 4.20 (d, J_{HH} = 12.70 Hz, 1H; Ar-CH_2-N), 4.37 (m, 1H; -CH_2-N), 4.60 (d, J_{HH} = 14.65 Hz, 1H; Ar-CH_2-N), 6.62–7.03 (m, 6H; ArH); ^{19}F NMR (360 MHz, $CDCl_3$): δ = −122, 126 (2F, ArF); MS (EI): *m/z* (%): 476 (100) $[M]^+$; IR (KBr; Mo=O): $\tilde{\nu}$ = 880 (s), 910 cm^{-1} (s); elemental analysis calcd (%) for $MoC_{19}H_{20}F_2N_2O_4$: C 48.11, H 4.25, N 5.91; found: C 48.15, H 4.39, N 6.30.

[MoO_2(L6)] (6): The complex was purified in an analogous manner to **2**. Yield: 0.27 g (53%); ^{1}H NMR (360 MHz, $CDCl_3$): δ = 1.25 (m, 2H; -CH_2-), 2.0 (m, 1H; -CH_2-N), 2.35 (m, 1H; -CH_2-N), 2.60 (m, 1H; -CH_2-N), 3.40 (d, 1H; J_{HH} = 12.15, Ar-CH_2-N), 3.60 (d, J_{HH} = 14.78 Hz, 1H; Ar-CH_2-N), 3.67 (m, 1H; -CH_2-N), 3.75 (m, 1H; -CH_2-N), 3.95 (m, 2H; -CH_2-N), 4.10 (d, J_{HH} = 12.25 Hz, 1H; Ar-CH_2-N), 4.38 (m, 1H; -CH_2-N), 4.60 (d, J_{HH} = 14.68 Hz, 1H; Ar-CH_2-N), 6.86–7.29 ppm (m, 6H; ArH); MS (EI): *m/z* (%): 508 (100) $[M]^+$; IR (KBr; Mo=O): $\tilde{\nu}$ = 886 (s), 912 cm^{-1} (s); elemental analysis calcd (%) for $MoC_{19}H_{20}Cl_2N_2O_4$: C 44.99, H 3.97, N 5.52; found: C 44.71, H 4.02, N 5.78.

Catalytic oxygen-atom-transfer reactions: Deuterated dimethyl sulfoxide ([D_6]DMSO) (1 mL) was added to the dioxomolybdenum(VI) complex (0.025 mmol) and PMe_3 (0.25 mmol) in the glove box at room temperature, and the mixture was stirred vigorously for 2 min to ensure complete dissolution. An aliquot of the reaction solution was placed in the NMR spectrometer, which had been preheated to 65 °C. The ^{31}P NMR spectra were recorded every 5 min.

Single-crystal X-ray data collection and structure solution: Single crystals of **1**–**4** of suitable size were selected from the mother liquor and immersed in paraffin oil, then mounted on the tip of a glass fiber. Data for the crystals were collected using $Mo_{K\alpha}$ (λ = 0.71073 Å) radiation on a Bruker SMART APEX 2 diffractometer equipped with a CCD area detector at 100 K. The crystallographic data are collected in Table 1. The APEX II[53] program was used for collecting frames of data, indexing reflections, and determining lattice parameters. The SAINT[53] program was used for integration of the intensity of reflections and scaling, the SADABS[54] program for absorption correction, and the WINGX[55] suite of programs for space group and structure determination, and least-squares refinements on F^2. The structure was solved by direct methods (SIR-92).[56] The other non-hydrogen atoms were located in successive difference Fourier syntheses. The final refinement was performed by full-matrix least-squares analysis. Hydrogen atoms attached to the ligand moiety were fixed in calculated positions and allowed to refine isotropically. CCDC-771525, 775228, 775229, 775230, and 775231 contain the supplementary crystallographic data for this paper. These data can be obtained free of charge from The Cambridge Crystallographic Data Centre via www.ccdc.cam.ac.uk/data_request/cif.

Computational methodology: The theoretical model system chosen in this work consists of the corresponding molybdenum catalyst, PMe_3 as a model substrate, and Me_2SO as oxidation reagent to close the catalytic cycle. All geometries were optimized in the gas phase by the B3LYP[57,58] DFT method, as implemented in TURBOMOLE.[59] Analytical harmonic frequency calculations for ZPE correction, as well as Mulliken Population Analysis (MPA) and Natural Population Analysis (NPA), were performed for all stationary points within the catalytic cycle. The results reported were obtained with a standard double-ζ quality basis set (def2-SVP) for all atoms except Mo, for which an effective core potential (ecp-28-mwb) with a corresponding double-ζ quality basis set (ecp-28-mwb-SVP) was used. Further calculations at selected stationary points with a basis set of higher quality, as well as solution-phase calculations using the COSMO model, did not lead to a significant change in energy differences.

Acknowledgements

Financial support by the Austrian Science Foundation FWF (P19309-N19) is gratefully acknowledged.

[1] Y. Zhang, V. N. Gladyshev, *J. Mol. Biol.* **2008**, *379*, 881–899.
[2] J. R. Turnlund, *Met. Ions Biol. Syst.* **2002**, *39*, 727–739.
[3] C. Feng, G. Tollin, J. H. Enemark, *Biochim. Biophys. Acta Proteins Proteomics* **2007**, *1774*, 527–539.
[4] J. H. Enemark, C. G. Young, *Adv. Inorg. Chem.* **1993**, *40*, 1–88.
[5] R. Hille, *Biochim. Biophys. Acta Bioenerg.* **1994**, *1184*, 143–169.
[6] R. Hille, *Chem. Rev.* **1996**, *96*, 2757–2816.
[7] R. Hille, J. Rétey, U. Bartlewski-Hof, W. Reichenbecher, B. Schink, *FEMS Microbiol. Rev.* **1998**, *22*, 489–501.
[8] C. Kisker, H. Schindelin, A. Pacheco, W. A. Wehbi, R. M. Garrett, K. V. Rajagopalan, J. Enemark, D. C. Rees, *Cell* **1997**, *91*, 973–983.
[9] a) H. Schindelin, C. Kisker, J. Hilton, K. V. Rajagopalan, D. C. Rees, *Science* **1996**, *272*, 1615–1621; b) M. J. Romao, M. Archer, I. Moura, J. J. Moura, J. LeGall, R. Engh, M. Schneider, P. Hof, R. Huber, *Science* **1995**, *270*, 1170–1176.
[10] G. N. George, C. A. Kipke, R. C. Prince, R. A. Sunde, J. H. Enemark, S. P. Cramer, *Biochemistry* **1989**, *28*, 5075–5080.
[11] G. N. George, R. M. Garrett, R. C. Prince, K. V. Rajagopalan, *J. Am. Chem. Soc.* **1996**, *118*, 8588–8592.
[12] R. M. Garrett, K. V. Rajagopalan, *J. Biol. Chem.* **1996**, *271*, 7387–7391.
[13] A. K. Rappe, W. A. Goddard, Jr., *J. Am. Chem. Soc.* **1982**, *104*, 3287–3294.
[14] A. V. Astashkin, C. Feng, A. M. Raitsimring, J. H. Enemark, *J. Am. Chem. Soc.* **2005**, *127*, 502–503.
[15] J. Enemark, J. J. A. Cooney, J. J. Wang, R. H. Holm, *Chem. Rev.* **2004**, *104*, 1175–1200.
[16] H. Sugimoto, H. Tsukube, *Chem. Soc. Rev.* **2008**, *37*, 2609–2616.
[17] B. S. Lim, K. M. Sung, R. H. Holm, *J. Am. Chem. Soc.* **2000**, *122*, 7410–7411.

[18] B. S. Lim, R. H. Holm, *J. Am. Chem. Soc.* **2001**, *123*, 1920–1930.
[19] B. S. Lim, M. W. Willer, M. Miao, R. H. Holm, *J. Am. Chem. Soc.* **2001**, *123*, 8343–8349.
[20] a) H. Sugimoto, K. Suyama, K. Sugimoto, H. Miyake, I. Takahashi, S. Hirota, S. Itoh, *Inorg. Chem.* **2008**, *47*, 10150–10157; b) H. Sugimoto, M. Tarumizu, H. Miyake, H. Tsukube, *Eur. J. Inorg. Chem.* **2006**, 4494–4497; c) H. Sugimoto, M. Harihara, M. Shiro, K. Sugimoto, K. Tanaka, H. Miyake, H. Tsukube, *Inorg. Chem.* **2005**, *44*, 6386–6392; d) H. Sugimoto, S. Tatemoto, K. Suyama, H. Miyake, S, Itoh, C. Dong, J. Yang, M. Kirk, *Inorg. Chem.* **2009**, *48*, 10581–10590.
[21] C. Schulzke, *Dalton Trans.* **2005**, 713–720.
[22] J. M. Berg, R. H. Holm, *J. Am. Chem. Soc.* **1985**, *107*, 925–932.
[23] J. M. Berg, R. H. Holm, *J. Am. Chem. Soc.* **1985**, *107*, 917–925.
[24] a) R. S. Sengar, V. N. Nemykin, P. Basu, *J. Inorg. Biochem.* **2008**, *102*, 748–756; b) A. J. Millar, C. J. Doonan, P. D. Smith, V. N. Nemykin, P. Basu, C. G. Young, *Chem. Eur. J.* **2005**, *11*, 3255–3267; c) Z. Xiao, M. A. Bruck, J. H. Enemark, C. G. Young, A. G. Wedd, *Inorg. Chem.* **1996**, *35*, 7508–7515.
[25] K. Most, S. Köpke, F. Dall′Antonia, N. C. Mösch-Zanetti, *Chem. Commun.* **2002**, 1676–1677.
[26] K. Most, J. Hobbach, D. Vidovic, J. Magull, N. C. Mösch-Zanetti, *Adv. Synth. Catal.* **2004**, *346*, 463–472.
[27] G. Lyashenko, R. Herbst-Irmer, V. Jancik, A. Pal, N. C. Mösch-Zanetti, *Inorg. Chem.* **2008**, *47*, 113–120.
[28] G. Lyashenko, G. Saischek, A. Pal, R. Herbst-Irmer, N. C. Mösch-Zanetti, *Chem. Commun.* **2007**, 701–703.
[29] C. J. Hinshaw, G. Peng, R. Singh, J. T. Spence, J. H. Enemark, M. Bruck, J. Kristofzski, S. L. Merbs, R. B. Ortega, P. A. Wexler, *Inorg. Chem.* **1989**, *28*, 4483–4491.
[30] a) J. Topich, J. T. Lyon III, *Inorg. Chim. Acta* **1983**, *80*, L41L43; b) J. Topich, J. T. Lyon III, *Polyhedron* **1984**, *3*, 61–65; c) J. Topich, J. T. Lyon III, *Inorg. Chem.* **1984**, *23*, 3202–3206; d) J. Topich, J. T. Lyon III, *Polyhedron* **1984**, *3*, 55–60.
[31] a) Y.-L. Wong, J.-F. Ma, W.-F. Law, Y. Yan, W.-T. Wong, Z.-Y. Zhang, T. C. W. Mak, D. K. P. Ng, *Eur. J. Inorg. Chem.* **1999**, 313–321; b) Y.-L. Wong, Y. Yan, E. S. H. Chan, Q. Yang, T. C. W. Mak, D. K. P. Ng, *J. Chem. Soc. Dalton Trans.* **1998**, 3057–3064.
[32] A. Lehtonen, R. Sillanpää, *Polyhedron* **2005**, *24*, 257–265.
[33] G. C. Tucci, J. P. Donahue, R. H. Holm, *Inorg. Chem.* **1998**, *37*, 1602–1608.
[34] P. D. Smith, A. J. Millar, C. G. Young, A. Ghosh, P. Basu, *J. Am. Chem. Soc.* **2000**, *122*, 9298–9299.
[35] a) A. A. Eagle, L. J. Laughlin, C. G. Young, E. R. T. Tiekink, *J. Am. Chem. Soc.* **1992**, *114*, 9195–9197; b) L. J. Laughlin, A. A. Eagle, G. N. George, E. R. T. Tiekink, C. G. Young, *Inorg. Chem.* **2007**, *46*, 939–948.
[36] a) W. B. Cross, J. C. Anderson, C. Wilson, A. J. Blake, *Inorg. Chem.* **2006**, *45*, 4556–4561; b) V. C. Gibson, A. J. Graham, M. Jolly, J. P. Mitchell, *Dalton Trans.* **2003**, 4457–4465; c) R. Ramnauth, S, Al-Juaid, M. Motevalli, B. C. Parkin, B. C, A. C. Sullivan, *Inorg. Chem.* **2004**, *43*, 4072–4079; d) W. B. Cross, J. C. Anderson, C. S. Wilson, *Dalton Trans.* **2009**, 1201–1205.
[37] R. Mayilmurugan, H. S. Evans, M. Palaniandavar, *Inorg. Chem.* **2008**, *47*, 6645–6658.
[38] D.-H. Jo, Y. M. Chiou, L. Que, Jr., *Inorg. Chem.* **2001**, *40*, 3181–3190.
[39] C. J. Whiteoak, G. J. P. Britovsek, V. C. Gibson, A. J. P. White, *Dalton Trans.* **2009**, 2337–2344.
[40] J. E. Ziegler, G. Du, P. E. Fanwick, M. M. Abu-Omar, *Inorg. Chem.* **2009**, *48*, 11290–11296.
[41] R. Mayilmurugan, E. Suresh, H. S. Evans, M. Palaniandavar, *Dalton Trans.* **2009**, 5101–5114.
[42] R. Mayilmurugan, PhD thesis, Bharathidasan University (India).
[43] E. Y. Tshuva, I. Goldberg, M. Kol, Z. Goldschmidt, *Organometallics* **2001**, *20*, 3017–3028.
[44] M. E. Judmaier, A. Wallner, G. N. Stipicic, K. Kirchner, J. Baumgartner, F. Belaj, N. C. Mösch-Zanetti, *Inorg. Chem.* **2009**, *48*, 10211–10221.
[45] B. E. Schultz, S. F. Gheller, M. C. Muetterties, M. J. Scott, R. H. Holm, *J. Am. Chem. Soc.* **1993**, *115*, 2741.
[46] L. M. Thomson, M. B. Hall, *J. Am. Chem. Soc.* **2001**, *123*, 3995–4002.
[47] P. Basu, V. N. Nemykin, R. S. Sengar, *Inorg. Chem.* **2009**, *48*, 6303–6313.
[48] Z. Xiao, M. A. Bruck, C. Doyle, J. H. Enemark, C. Grittini, R. W. Gable, A. G. Wedd, C. G. Young, *Inorg. Chem.* **1995**, *34*, 5950–5962.
[49] A. J. Millar, C. J. Doonan, L. J. Laughlin, E. R. T. Tiekink, C. G. Young, *Inorg. Chim. Acta* **2002**, *337*, 393–406.
[50] A. J. Bard, L. R. Faulkner, *Electrochemical Methods: Fundamental and Applications*, Wiley, New York, **1980**, p. 218.
[51] C. J. Doonan, D. A. Slizys, C. G. Young, *J. Am. Chem. Soc.* **1999**, *121*, 6430–6436.
[52] B. W. Kail, L. M. Pérez, S. D. Zaric, A. J. Millar, C. G. Young, M. B. Hall, P. Basu, *Chem. Eur. J.* **2006**, *12*, 7501–7509.
[53] SAINTPLUS, Software Reference Manual, Version 6.45, Bruker-AXS, Madison, I, **1997–2003**.
[54] R. H. Blessing, *Acta Crystallogr. Sect. A* **1995**, *51*, 33–38. SADABS, version 2.1, Bruker-AXS: Madison, WI, **1998**.
[55] L. J. Farrugia, *J. Appl. Crystallogr.* **1999**, *32*, 837–838.
[56] A. Altomare, G. Cascarano, A. Gualardi, *J. Appl. Crystallogr.* **1993**, *26*, 343–350.
[57] A. D. Becke, *J. Chem. Phys.* **1993**, *98*, 5648–5653.
[58] C. Lee, W. Yang, R. G. Parr, *Phys. Rev. B* **1988**, *37*, 785–789.
[59] TURBOMOLE V6.0.2 2009, a development of University of Karlsruhe and Forschungszentrum Karlsruhe GmbH, 1989–2007, TURBOMOLE GmbH, since 2007, available from http://www.turbomole.com.

Received: May 3, 2010
Revised: August 27, 2010
Published online: November 12, 2010

